Hertzian contact transducers for nondestructive evaluation

F. L. Degertekin and B. T. Khuri-Yakub
Stanford University, E. L. Ginzton Laboratory, Stanford, California 94305

(Received 29 August 1994; accepted for publication 5 July 1995)

Hertzian, dry, pointlike contacts are used to couple ultrasonic energy efficiently to plate wave modes in anisotropic solid plates. A new transducer configuration using a piezoelectric PZT-5H transducer and a quartz buffer rod is realized for this purpose. In particular, the lowest order antisymmetric Lamb wave ($A0$) mode is excited and detected in anisotropic plates at a frequency of 200 kHz and with signal-to-noise levels exceeding 65 dB. Time delay measurements and FFT techniques are used to obtain dispersion and anisotropy curves of phase velocity in anisotropic plates. The accuracy of the method is limited mainly by the distance measurements. In (001) silicon plates the agreement between theory and experiments is obtained with an accuracy of $\pm 0.08\%$. Anisotropic phase velocity measurements are also performed for uniaxial graphite/epoxy composite plates and the results are compared with the theoretical model to derive the elastic constants of the composite. Through accurate phase velocity measurements, it is possible to detect delamination defects in composite plates with high resolution operating at 200 kHz. Using the surface impedance approach, a model is also developed to predict the effects of delaminations on phase velocity and the results are verified by experiments.

PACS numbers: 43.35.Zc, 43.35.Yb, 43.38.Ar, 43.60.Qv

INTRODUCTION

Ultrasonic methods are widely used for the nondestructive evaluation (NDE) of anisotropic solids, since they reveal the mechanical properties and internal structure.[1] Phase velocity measurement of different modes is one of the most common of these methods utilized to provide information about the elastic constants, density, and various structural features of materials.[2] Accurate, absolute measurements of wave velocity, especially in industrial applications that do not permit special sample preparation, is still a topic of challenging research. This paper presents a flexible, dry, nondestructive method for efficient excitation and detection of ultrasonic waves in solid plates through a Hertzian contact. As a particular application to nondestructive evaluation, accurate phase velocity measurements and delamination detection in a uniaxial composite plate are presented and the results are compared to theoretical predictions.

With their growing number of applications, composite structures have become an important subject of ultrasonic inspection methods. Especially, investigations are conducted for material properties determination and detection of defects such as delaminations, cracks, misalignment of fibers, etc.[3] Lamb waves are the dominantly used ultrasonic wave modes for nondestructive evaluation of solid plates. A common method to excite Lamb waves in composite plates is by mode conversion of an ultrasonic longitudinal wave incident in a coupling liquid onto the sample. By adjusting the frequency and incidence angle, a particular leaky wave mode can be excited efficiently.[4–6] Transmission and reflection of the leaky waves are then used for velocity determination and defect detection. By mechanical scanning, it is also possible to obtain images of the sample.[7] However, wetting the sample is undesirable, and the immersion requirement results in problems for practical applications such as measurements at high temperatures and in clean environments.

Generation and detection of ultrasonic waves using lasers provide a noncontacting means for nondestructive evaluation in different environments.[8–15] Using different interferometric or probe beam deflection schemes it is possible to detect small displacements.[9,10] Generation of ultrasonic waves using laser beams with sufficient amplitude for accurate measurements requires special sample preparation.[8] These methods include film deposition on the sample surface to enhance the thermoelastic interaction by vaporizing the film material,[11] or painting the region of excitation to increase the light absorption.[12] Using a laser ultrasound system, surface wave velocity measurement with accuracy in the order of 0.001% is possible.[12] In this case, however, an optically polished, perfectly flat sample is used and the surface of the sample is painted to increase optical absorption. Also, the reflections due to finite sample size should be prevented by acoustic absorbers since a continuous-wave excitation technique is used.[12] These sample conditions are not easy to meet in practical cases such as composite plates, which have finite size and surface roughness.

Point source–point receiver (PS–PR) methods are mostly used to accurately measure wave velocities of anisotropic solids.[16,17] Focused laser beams, small aperture piezoelectric transducers, or glass fractures are used as pointlike sources. Capacitive and piezoelectric transducers much smaller than the wavelength of propagation are used as point receivers. These current PS–PR techniques require surface preparation, single use sources, and ultrasonic transducers that are permanently bonded to the sample.[16,17]

An elastic Hertzian contact between two solid media creates a boundary through which acoustic energy can be coupled efficiently. This phenomenon has found several applications. Using the Hertzian contact between a glass capillary and an optical fiber, it is possible to achieve acousto-

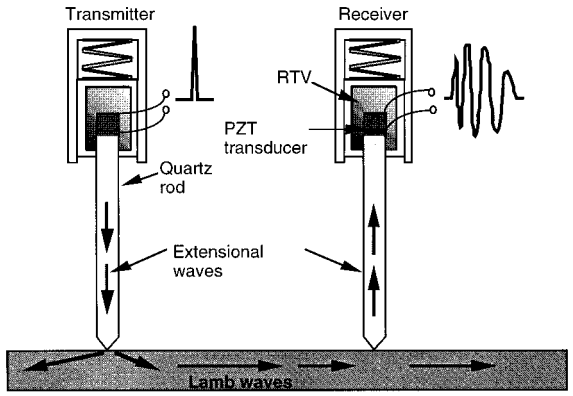

FIG. 1. Schematic of Hertzian contact transducer system with quartz rod and PZT-5H transducer material. The housing is filled with RTV (room-temperature vulcanizing) rubber. The transducers are spring loaded to have repeatable force applied on contact.

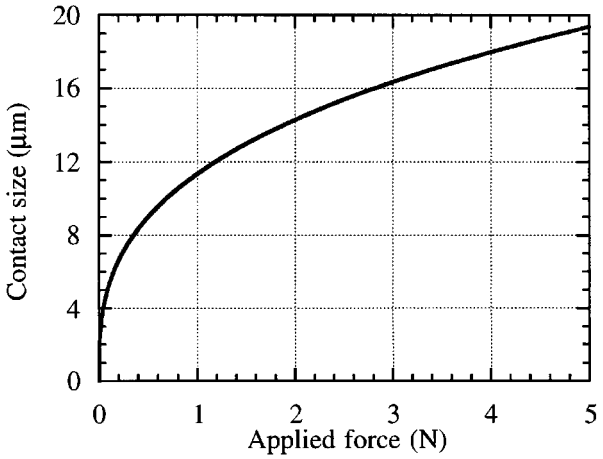

FIG. 2. Radius of Hertzian contact formed between a fused-quartz sphere of radius 100 μm and a planar silicon sample as a function of applied force. Isotropic elastic constants are used for silicon.

optic modulation at 1 GHz.[18] In another application, spherical resonances of bulk and surface waves are excited in ceramic bearing balls using a single point Hertzian contact with an acoustic lens having a large diameter, and the displacements are detected by an optical heterodyne interferometer in the frequency range of 30–70 MHz.[15] Inspection of the resonances provides information about material properties and the defects in the ceramic balls.

In this study, a PS–PR technique using acoustic energy coupling by pointlike Hertzian contacts formed between a specially shaped buffer rod and the sample is proposed for accurate phase velocity measurement of various ultrasonic modes. The method has the efficiency of piezoelectric transducers yet it does not require any permanent bonding or liquid coupling medium and can be used in clean and high-temperature environments. The transducer geometry is depicted in Fig. 1. Extensional waves, generated in a transmitter buffer rod by a piezoelectric cylinder, are coupled to the ultrasonic modes in the solid and detected by a similar transducer at another location. The geometry of the tip of the buffer rod and the applied force can be adjusted to insure a repeatable point contact of particular size with the sample. Spring loading enables the transducers to be used on contoured samples. With this configuration, time delay and frequency spectrum measurements can be employed to measure phase velocity with a signal-to-noise ratio exceeding 65 dB. In many cases, we call such transducers ''noncontacting'' because most samples under test are not levitated. Thus ultrasonic waves can be coupled in and out of a sample without an additional contact other than the already existing support contacts.

In this paper, we present the results of Hertzian contact theory used to calculate the pointlike source/receiver size of the transducers. A brief summary of Lamb wave propagation characteristics in solid plates is also presented. Next, we describe the transducers and discuss the experimental measurement methods. Optical probe beam deflection measurements are used to investigate and confirm the repeatability and elastic nature of the contact. Material characterization results obtained for single-crystal silicon and uniaxial graphite/epoxy composite plates are presented later. Finally, an application of the technique for detecting delamination in composite plates is discussed and experimental results are compared with theory.

I. THEORY

A. Hertzian contact as a point source

The problem of the elastic contact between two solid media was first solved by Hertz.[19] Two solid bodies in contact under the application of force deform elastically and form a flat contact region, the so-called Hertzian contact. The contact does not result in permanent deformation, and can be used for ultrasonic energy transmission without any coupling medium. The use of Hertzian contact for this purpose has been demonstrated.[15,18] Since the ultrasonic energy is coupled through the contact, the contact size is then the aperture size of the source (or receiver). For two isotropic solids with spherical shapes, and with radii R_1 and R_2, the contact has a circular shape with radius a, which can be calculated as

$$a = F^{1/3}\left(\frac{DR_1R_2}{(R_1+R_2)}\right)^{1/3}, \tag{1}$$

where

$$D = \frac{3}{4}\left(\frac{1-\sigma_1^2}{E_1}+\frac{1-\sigma_2^2}{E_2}\right),$$

E_1 and E_2 are Young's moduli, σ_1 and σ_2 are Poisson's ratios of the two media, respectively, and F is the force applied to the contact.[19] For a given material pair, the contact size is determined by the geometry and applied force, which can be adjusted for a specific application. The size of the Hertzian contact formed between a fused-quartz sphere with 100-μm radius and a planar ($R_2=\infty$) composite sample is plotted as a function of applied force in Fig. 2. These are the typical materials and geometrical values used in our experiments. The repeatability, and hence the elasticity of the Hertzian contact, is investigated using the probe beam deflection technique and the results are discussed in the following sections. For a typical applied force of 2 N, the radius of contact is

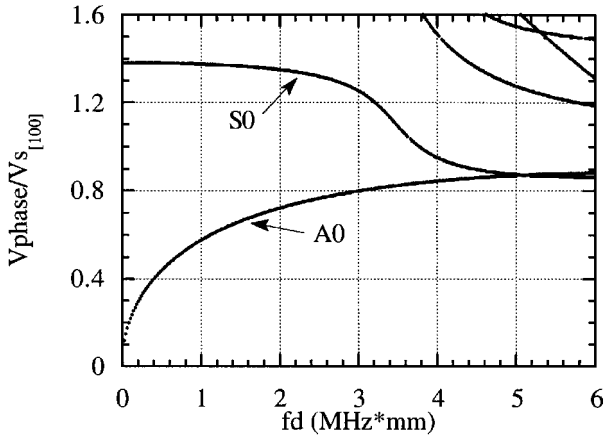

FIG. 3. Dispersion curves for the Lamb wave modes for a (001) silicon plate in the [100] direction. The phase velocity is normalized by the shear wave velocity in [100] direction.

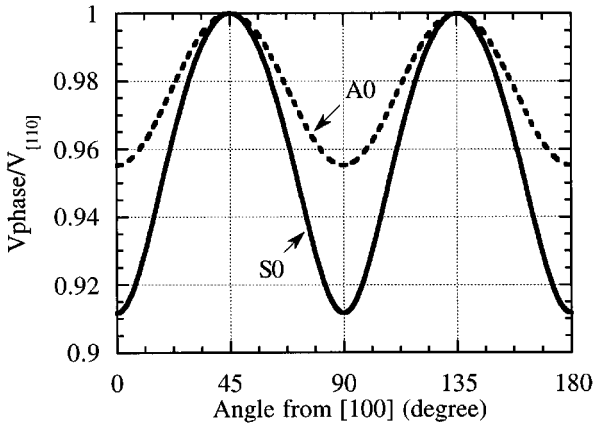

FIG. 4. Variation of normalized phase velocity of lowest order Lamb waves in (001) silicon plate, $fd=0.056$.

around 15 μm. In our experiments, the dominant mode of ultrasonic propagation is the $A0$ mode which has a phase velocity in the range of 900–1600 m/s around 200 kHz. This results in a wavelength $\lambda\sim 4.5-8$ mm, which is more than two orders of magnitude larger than the contact size. Thus the Hertzian contact can safely be assumed to approximate a PS–PR for practical purposes. The small aperture size enables precise distance determination for absolute velocity measurements and eliminates the diffraction errors, as will be discussed in the following sections.

B. Lamb waves in solid plates

Lamb waves are elastic wave modes propagating in solid plates with free boundaries. They propagate in the plate as a proper combination of longitudinal and shear waves.[20,21] In a plate of a certain thickness, a finite number of Lamb wave modes can propagate depending on the frequency of operation. For an isotropic plate, the solutions of the so-called Rayleigh–Lamb equations give the phase velocity of Lamb waves as a function of frequency–thickness product ($fd=f^*d$). For anisotropic plates, the solutions should simultaneously satisfy the Christoffel's equations and the free-boundary conditions to give the propagation direction-dependent phase velocity.[22] In both cases, the Lamb wave modes are separated as symmetric or antisymmetric depending on the variation of the particle displacement component in the propagation direction along the thickness of the plate. Figure 3 depicts the phase velocity variation of Lamb wave modes in a (001) silicon plate in the [100] direction, as a function of fd. All of these modes, except the lowest order symmetric ($S0$) and antisymmetric ($A0$) modes, have lower cutoff frequencies. This feature makes $A0$ and $S0$ modes interesting since they can be chosen as the only modes of propagation in a PS–PR experiment. The phase velocity of the $S0$ mode is close to the extensional wave velocity and is nearly constant for $fd<2$ MHz mm. In contrast, the phase velocity of the $A0$ mode is highly dispersive in that region with phase velocity going to very small values as $fd\rightarrow 0$. As fd gets larger both modes converge to the Rayleigh surface wave in the limit. Anisotropy of the solid plate results in direction-dependent phase velocity for these modes. The calculated phase velocity variation of $A0$ and $S0$ modes in a (001) silicon plate for $fd=0.056$ MHZ mm is depicted in Fig. 4. The velocity is normalized to the phase velocity in the fastest [110] direction. The anisotropy of the $S0$ mode is about 9% whereas that of the $A0$ mode is 4.5%, with both modes showing the expected fourfold symmetry around the Z axis.

II. EXPERIMENTAL METHODS

When a particle displacement at a certain frequency is introduced at the surface of a solid plate, all the Lamb wave modes are excited. But only those modes whose resonance frequencies are matched can propagate, whereas the modes with higher cutoff and nonmatched resonances are evanescent. To have a single Lamb wave mode propagation, the frequency and nature of the excitation should be chosen properly. For the sample plates used in this study, the frequency of operation, determined by the transducer characteristics, is chosen below the cutoff frequencies of the higher-order modes. Furthermore, due to the antisymmetric nature of the setup used, i.e., the transmitter and receiver contacting only one side of the sample, no symmetric modes are excited or detected. Virtually, single mode operation with the $A0$ mode is possible. Since the $A0$ mode propagates as a combination of shear and longitudinal waves, its propagation characteristics are determined by the bulk elastic constants and the structural properties of the plate. So, accurate measurements of the dispersion and anisotropic properties of this mode provide crucial information for material characterization and defect detection.[23] Both measurements are performed successfully using the Hertzian contact transducers.

Hertzian contacts are used to couple ultrasonic energy to the $A0$ mode in the samples. Ultrasonic transducer materials cannot be used directly to form repeatable Hertzian contacts in many environments, because of temperature, contamination, and surface roughness problems. For these reasons fused quartz is used as a buffer medium between the piezoelectric transducer and the sample. The geometry of such a Hertzian contact transducer is depicted in Fig. 1. Cylindrical PZT-5H transducers, 5 mm in thickness, are epoxy bonded to

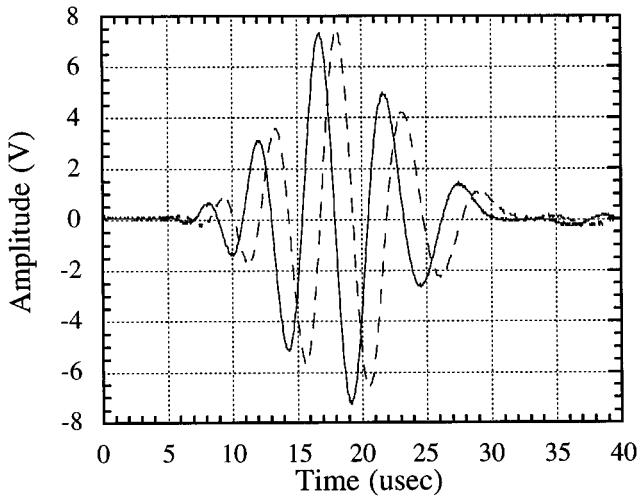

FIG. 5. Received waveforms for a 0.28-mm-thick (100) silicon plate in the [110] direction for two receiver locations 1.25 mm apart. The transmitter–receiver distance is 2.54 cm.

quartz rods 3 mm in diameter and 14.7 cm long. In this configuration, the transducer has a 40% bandwidth centered at 200 kHz in the thickness mode. The other end of the rods is sharpened to induce larger displacements, and the tips are spherically shaped with a 100-μm radius of curvature and polished by mechanical means. This geometry results in repeatable pointlike Hertzian contacts with the samples. The piezoelectric part of the transducers is placed in an RTV filled aluminum housing to prevent contamination in a clean environment and for ease of handling. To excite ultrasonic waves in samples, an electrical pulse is applied to the terminals of the piezoelectric transducer which in turn generates extensional waves guided in the quartz rod. At the Hertzian contact between the sample and the tip of the quartz rod, the displacements induced by extensional waves are coupled to the $A0$ mode in the plate.

Two such transducers are spring loaded and placed on a vertical translation stage which is used to control the applied force with the help of a micrometer. One of the transducers is placed on another micrometer stage to allow measurements with different source–receiver spacings. Sample plates are placed on a holder with a tilt stage for alignment and a rotation stage for anisotropy measurements. A Panametrics 5055 pulser is used to excite the transmitter with a wideband 130-V peak pulse for dispersion measurements. For single frequency phase velocity anisotropy measurements, tone bursts of ten cycles with 30-V peak amplitude are applied. A low noise JFET preamplifier is attached directly to the receiver transducer for minimum noise corruption. With a 1-N force applied to the contact, an SNR of better than 55 dB is achieved at the receiver end while working with silicon samples. Higher signal-to-noise ratios are possible with larger forces. Typical output waveforms with pulse excitation at two different receiver locations are shown in Fig. 5. The output signal is fed to a Stanford Research Systems SR620 precision time interval counter for time delay measurements. This signal is also digitized by a Tektronix 2430A oscilloscope with 8-bit resolution for dispersion calculations using FFT techniques in a digital computer.

The repeatability of the Hertzian contact is tested using a probe beam detector to monitor the displacement on the sample surface. A 4-mW He–Ne laser is directed on the surface of the polished silicon plates and the reflected beam is detected using a bicell photo detector. The output signal of the detector is amplified by 60 dB using a low noise amplifier. This signal is proportional to the spatial derivative of the surface displacement.[10] The bicell detector is assured to work in the linear regime during the measurements by adjusting the voltage of the input pulse to the transducer. Lamb wave propagation in the plates and the repeatability of the Hertzian contact are tested by comparing the detector output waveforms.

Since the $A0$ mode is highly dispersive in the low fd region, the measurement of the dispersion curve becomes an important tool for material characterization.[24,25] For this purpose, a wideband pulse is used in to excite the full bandwidth of the transducers. Signals are collected at two locations, in the same direction, and with a distance resulting in a phase difference of less than 2π. FFT routines are used to get the phase of these two detected signals in the frequency domain. After the phase is unwrapped, the frequency-dependent phase velocity is calculated using the relation

$$V_p(f) = \frac{2\pi f \Delta d}{\Delta \phi(f)}, \tag{2}$$

where Δd is the distance between the two receiver locations, and $\Delta\phi(f)$ is the absolute value of the phase difference of the waveforms at frequency f. The accuracy of this technique is determined mainly by the phase errors resulting from trigger and clock jitter.[24] For the particular digitizing oscilloscope, the standard deviation of phase error is measured as 0.02 rad in the 3-dB bandwidth of the transducer, resulting in an estimated error of 0.6% in the phase velocity measurement. However, the unwrapping process introduces an accumulation of phase error depending on the bandshape of the system. Measurements indicate that for this particular digitizer–transducer pair, the maximum accumulated phase error is estimated as 0.07 rad at the lower edge of the passband, which corresponds to an uncertainty of 2.1% in phase velocity at the particular frequency. This error can be greatly reduced using a suitable digitizer.[24]

For anisotropic phase velocity determination at a single frequency, precise time delay measurements are carried out. In this case, to avoid the effect of dispersion the input signal should be as selective as possible in its frequency. For this purpose, the transmitter is excited by a long tone burst, which was limited by the length of the buffer rod. For a 14.7-cm-long quartz rod, the round trip time for the extensional wave is 53 μs, limiting the number of cycles to ten at 200 kHz. The phase velocity is then measured as follows: A particular zero crossing in the echo signal reflected from the tip of the transmitter is taken as the timing reference. The time delay between this reference and a particular zero crossing in the received signal is measured with 25-ps resolution by the time interval counter. The time delay measurement is repeated using the same zero crossing with the receiver lo-

the contact, to have a constant received signal amplitude. From the known distance and time delay difference, the phase velocity is calculated as $V_p = \Delta x/\Delta t$. As discussed in Appendix A, although the wave packet envelope propagates with the group velocity at that frequency, the individual zero crossings in the signal move with the phase velocity, where the envelope of the signal has a vanishing time derivative. This fact is easily observed in the experiments: Because of high dispersion, the group velocity of the $A0$ mode is approximately two times that of the phase velocity in the frequency range of interest.

The error in phase velocity measurement results from the uncertainty of time delay and distance measurements. Since the delay counter is very accurate and SNR is assured to be larger than 50 dB in all measurements by signal averaging at the counter when necessary, the resulting error in time delay measurements is on the order of 2×10^{-5}, assuming a minimum $\Delta t = 1.25$ μs and 25-ps resolution of the time delay counter.

The accuracy of the phase velocity measurements is determined dominantly by the source–receiver distance measurements. Although the transducers are mounted on mechanical micrometer stages, to enhance accuracy, optical inspection is used. Single side polished silicon wafers are coated by 5000-Å-thick photoresist films. These wafers are only prebaked at 90 °C for 20 min to have a soft film on the polished side. In the experiments, first, these dummy wafers with photoresist films are placed on the sample stage and the contact points are marked on the photoresist film by the indentations of transducer tips. The distances are then accurately determined by examining these marks under an optical microscope. The size of the Hertzian contact is also qualitatively verified by measuring the size of the indentations. By this method, the uncertainty in determining the distance between two receiver positions (Δx) for phase velocity measurements is reduced to less than 1 μm. The tips are cleaned before the measurements on the real samples are carried out.

The effect of diffraction in the measurements is very small due to the fact that the sizes of the source and receiver are very small as compared to the wavelength. As shown in Appendix B, the resulting error in phase velocity can be estimated to be on the order of 1×10^{-6} for typical Hertzian contact sizes. It should be noted that the anisotropy does not affect the results significantly since the angular span of rays between the transmitter and receiver is very small. The other effect of anisotropy is the directivity of energy, resulting in variation of amplitude levels with direction of measurement. By locating the receiving transducer at two different spacings in the same direction and keeping the amplitude constant for each measurement, this effect is eliminated. Hence, the error in absolute phase velocity determination is dominated by the accuracy of distance measurements, which is around $\pm0.08\%$. This figure is by no means a hard limit for the method; it is imposed by the particular experimental setup. cated at a different point on the propagation path. The amplitude of the input signal is adjusted rather than the force on

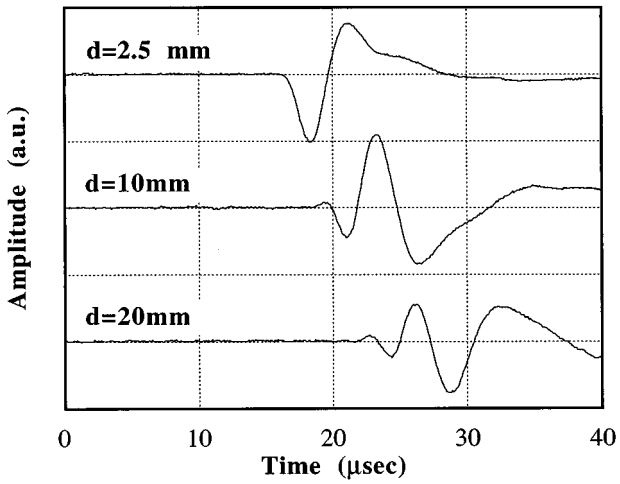

FIG. 6. Optical probe beam detector output for three different spacings between the probe point and the Hertzian contact in ⟨110⟩ direction. The sample is a 0.5-mm-thick (001) silicon plate. The signals for $d = 10$ mm and $d = 20$ mm are two times magnified.

III. RESULTS

A. Optical probe beam measurements for Hertzian contact characterization

To observe the propagation of the Lamb wave excited by the Hertzian contact transducer in the sample plates, a transducer with 100-μm tip radius is used as a transmitter with 1.2-N force applied to the contact. The sample is a (001) silicon plate with 0.5-mm thickness. In Fig. 6, the digitized single-shot detector output signals with the probe beam located at distances of 2.5, 10, and 20 mm to the Hertzian contact in the [110] direction are plotted. For the last two cases the signals are magnified two times for better comparison. The dispersive nature of the $A0$ mode is evident from the waveform distortion with increasing distance and the high SNR indicates the efficiency of excitation. Repeatability of the Hertzian contact is also tested using the same setup. For this purpose, the transducer is brought in contact with the sample numerous times with the same applied force of 1.2 N.

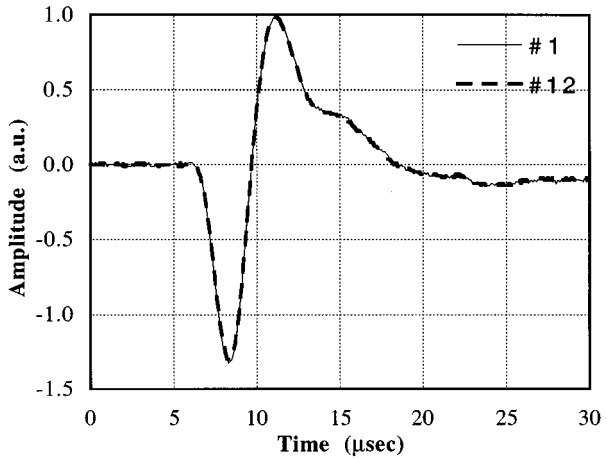

FIG. 7. Probe beam detector output waveforms obtained by the 1st and 12th applications of the Hertzian contact transducer with the probe distance of 2.5 mm.

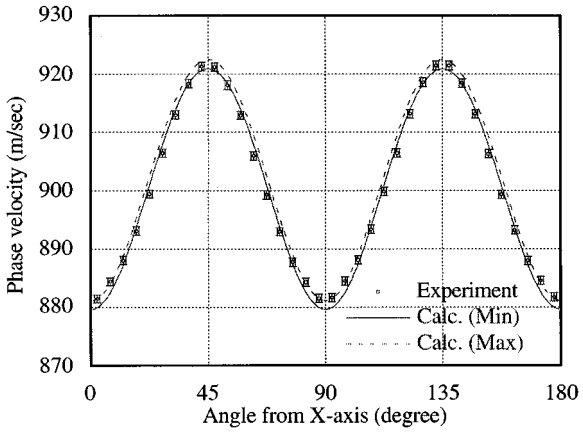

FIG. 8. Phase velocity variation of $A0$ mode in the same silicon sample in Fig. 4. The squares indicate experimental data with the error bars and the solid and dashed lines are the calculated extrema for anisotropic phase velocity.

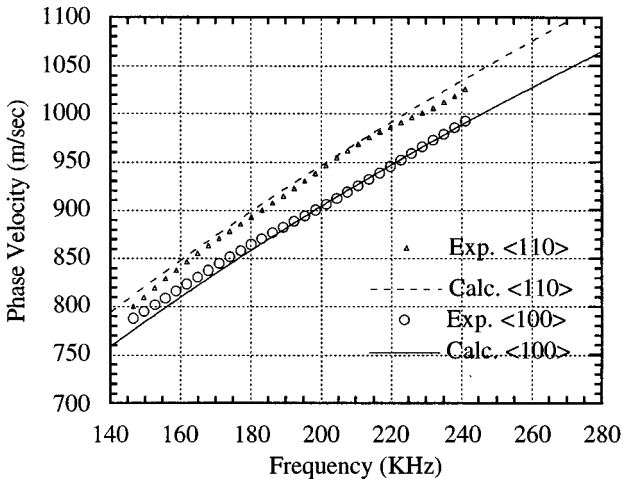

FIG. 9. Experimental and calculated dispersion curves for the silicon sample in two different propagation directions.

The peak-to-peak value of the detector signal is observed to vary less than 2%, which is probably due to the nonrepeatability of the spring mechanism. Two samples from the digitized signal ensemble obtained at a point 2.5 mm away from the contact point in the [110] direction are plotted with corresponding index numbers in Fig. 7. The consistent reoccurrence of these waveforms confirms that the Hertzian contact is repeatable and hence the resulting Hertzian contact transducer is elastic and nondestructive. Optical examination of sample surfaces also shows no indication of any plastic deformation.

B. Material characterization

Two different materials are characterized using the methods described earlier. Silicon is chosen as a test material because of its well characterized properties and availability in the form of wafers with perfect crystal structures.[21,26,27] A uniaxial fiber reinforced composite plate is also used in our experiments because of the importance of composite materials in many practical applications. For theoretical calculations of Lamb wave propagation in anisotropic plates a computer program using the boundary-condition approach is developed.[22]

The silicon sample is a (001) double side polished wafer. The wafer is ground down to a thickness of 0.28 mm to decrease the phase velocity and prevent interference with other Lamb wave modes. Both surfaces of the sample are then optically polished. The results of anisotropic phase velocity measurements at 200 kHz for this sample are depicted in Fig. 8. The angle is measured from the [100] direction in increments of $5°\pm0.5°$. The 0° angle is determined using the orientation flat provided by the semiconductor wafer manufacturer, which in this case is accurate to $\pm1°$. The SNR is measured as 55 dB at the receiving end in the slowest direction. In the same figure, the calculated phase velocities using the extremum values of reported elastic constants are also plotted showing a variation of $\pm0.1\%$. The experimental results with the error bars corresponding to the estimated $\pm0.08\%$ variation in phase velocity and $\pm0.5°$ uncertainty in angle measurements are also depicted. The fourfold symmetry with 4.6% variation in phase velocity of the $A0$ mode is observed as expected from Fig. 4. The agreement between the experimental results and calculated acceptable limiting values is as predicted and shows the efficacy of the method. Using the FFT method described, the dispersion curves for the same sample are measured in different directions. Figure 9 shows the results for [100] and [110] directions along with calculated dispersion curves. The effect of anisotropy is clearly observed and the agreement is good in the 3-dB bandwidth of the transducers. The error at the edges of the passband is around 2% as expected. With addition of another receive or transmit transducer at a fixed distance on the measurement path and using a better digitizer, this method can be used as a fast way for dispersion measurements.

The uniaxial composite sample used for characterization was made by stacking 12 plies of T300/976 graphite/epoxy material in the same orientation. The density and thickness of the plate are measured as 1510 kg/m^3 and 1.7 mm, respectively. Although the composite material does not have a regular crystal structure resulting in high attenuation as compared

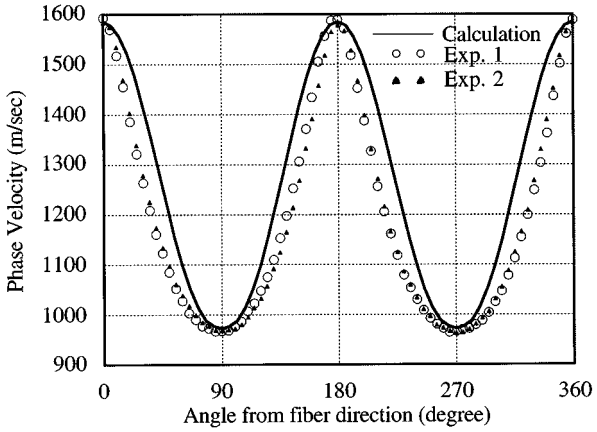

FIG. 10. Phase velocity variation of the $A0$ mode in a uniaxial composite plate of thickness 1.7 mm at 200 kHz. The circles and filled triangles are experimental data whereas the calculation is plotted as a solid line.

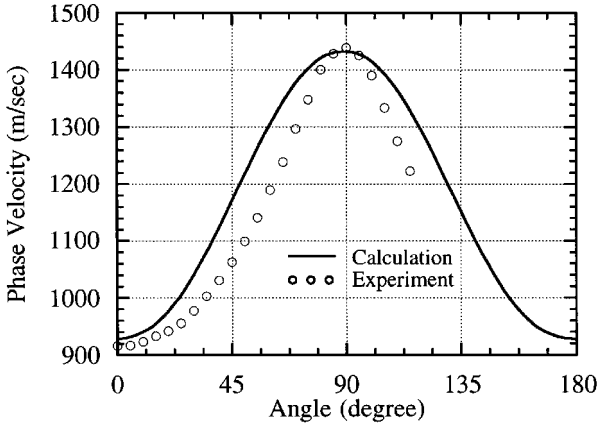

FIG. 11. Phase velocity variation with propagation direction for the $A0$ mode in the defective region. The angle is measured from the off-fiber axis. The circles represent the measured data and the solid line is the calculated curve.

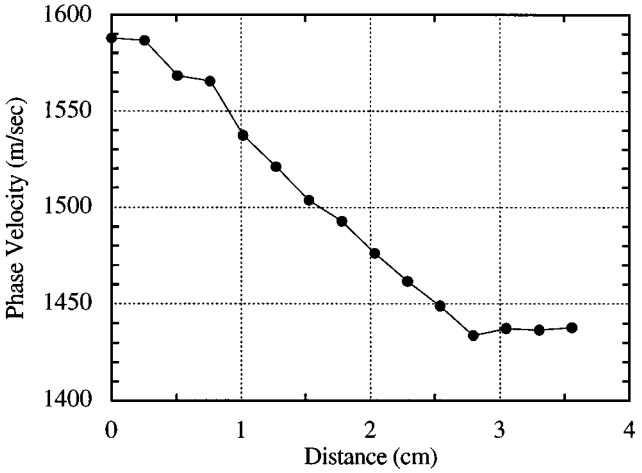

FIG. 12. Measured phase velocity variation data in the fiber direction during the line scan starting in the good region and ending in the delamination region.

to the silicon sample, SNR has been measured as 40.3 dB in the most attenuating direction (slowest). Averaging is used to overcome the problem of reduced SNR and enhance the accuracy of the measurements. For theoretical calculations, the transverse isotropy assumption is used with five independent elastic constants.[28] The measured and calculated angular dependence of the Lamb wave phase velocity at 200 kHz is depicted in Fig. 10. The propagation angle is again measured from the fiber axis with $5°\pm0.5°$ increments and the 0° is determined by the given fiber orientation. The nearly 60% variation in phase velocity results from the high anisotropy with twofold symmetry in this sample. The calculated curve is obtained by adjusting some of the elastic parameters in their tolerance range. Although the measured values agree reasonably well in the direction along and perpendicular to the fiber axis, there is a significant difference in other directions. To further confirm the measured values, the experiment is repeated on different regions of both the top and bottom surface of the sample and these measurements are also plotted in Fig. 10. It is clearly seen that the measured data is very consistent and repeatable considering the nonuniform surface conditions of the composite plate. Results indicate that the experimental data can be used to characterize the sample using some iterative algorithms to obtain a better agreement with calculations.[23]

C. Defect detection

Different kinds of defects such as delaminations and cracks occur during the manufacture and use of composite plates. The ultrasonic waves coupled to the solid structure interact with these defects, and changes in their amplitude and phase velocity are observed.[29] Since the Hertzian contact transducers enable accurate measurement of both quantities, it is also used for defect detection. A delamination defect is simulated by inserting a 6.4-cm^2, square-sized, 100-μm-thick Teflon layer at the middle plane of a composite plate.[30] The Teflon layer is suitable for this purpose since it introduces a large discontinuity in elastic properties for a very small thickness simulating a delaminated interface. The effect of this defect on the phase velocity is measured by moving both transmit and receive transducers over the defect region. Figure 11 depicts the phase velocity variation with propagation direction for defective regions which had no visible difference from the good region. The measured angle span is limited to 115° because of the limitations in the mechanical fixture. For theoretical calculations, a program using the surface impedance approach is developed that can handle Lamb wave propagation in general multilayered anisotropic materials without any numerical problems.[31] The calculated phase velocity values compare very well in the fiber and perpendicular to fiber directions. The elastic constants used in calculations are the same as for Fig. 10. A 10% phase velocity variation is observed in the phase velocity in the fiber direction resulting from the delamination defect. The Teflon layer effectively reduces the plate thickness, resulting in a lower phase velocity due to dispersion.

The effect of defect size on the phase velocity of the $A0$ mode is also investigated. For this purpose, the composite plate sample is placed on a micrometer stage to perform a line scan. The phase velocity in the fiber direction is measured while the sample is translated laterally, starting with both transducers in the good region and ending with both in the defective region. The phase velocity variation as a function of position for a 2.2-cm separation between the transmitter and receiver is plotted in Fig. 12. The phase velocity decreases approximately linearly with changing defect size included in the measurement path. The slope of this variation is 58.7 m/s per cm of defective region along the measurement path, in the case where the defect extends longer than a couple of wavelengths along the perpendicular direction. With the available 55-dB SNR resulting in a ±1-ns time delay accuracy, it is possible to detect relative phase velocity variations on the order of 1 m/s assuming constant spacing. Then, for this particular sample, using the linear relation between the defect size and velocity variation, the system enables detection of defects having one of its dimensions on the order of 10 μm. It should be noted that this sensitivity decreases with increasing transducer spacing and delamination depth.

IV. CONCLUSION

A nondestructive PS–PR method for material characterization and defect detection using ultrasonic waves is presented. Through the use of elastic Hertzian contacts, it is possible to excite and detect Lamb waves in anisotropic plates with high efficiency providing SNR levels exceed 50 dB. Using the method, anisotropic phase velocities of $A0$ modes are measured with $\pm 0.08\%$ uncertainty. Characterization of a uniaxial graphite/epoxy composite plate is performed and compared with calculations as an application. More importantly, delamination defects in composite plates are examined and high sensitivity is observed, in agreement with theoretical model. Line scan measurements on defective regions suggest that the method can detect delaminations with dimensions very small as compared to wavelength by $A0$ mode Lamb waves around 200 kHz.

The method is not limited to Lamb wave excitation at a limited frequency range, since the Hertzian contacts can be used as flexible displacement actuator/sensors to generate bulk and surface waves in solids as other PS–PR methods.[16,18] Since there is no coupling medium requirement, the method can be used in low-pressure, high-temperature, and clean environments, which makes it suitable for process monitoring. Also, using large number of transducers, tomographic imaging and array applications can be realized. Hand-held systems to be used on arbitrary sample geometries for defect inspection are also possible with proper mechanical designs.

ACKNOWLEDGMENTS

This research was supported by SRC under Contract No. SRC 94-YC-704. The authors are grateful to Jun Pei for the help in mechanical fixtures and Dr. B. Victor Honein for suggesting the surface impedance method for propagation calculations in multilayered solid plates. Dr. Fu-Kao Chang of the Aeronautics and Astronautics Department of Stanford University is thanked for the uniaxial composite samples. The authors greatly appreciate the helpful critique of an anonymous reviewer.

APPENDIX A: PHASE VELOCITY MEASUREMENT USING ZERO CROSSINGS

Assume the transmitting Herztian contact transducer is excited by a narrow-band electrical signal of the form

$$T(t)=Af(t)\cos(\omega_0 t) \tag{A1}$$

and the frequency-dependent propagation constant of the excited mode in the sample is given by $\beta(\omega)$. Then, at a distance x_0 from the transmitter, the signal at the receiving end can be written, to a first-order approximation, as

$$R(x_0,t)\cong Bf\left(t-\frac{x_0}{V_g}\right)\cos\left[\omega_0\left(t-\frac{x_0}{V_p}\right)+\psi\right], \tag{A2}$$

where the constants B and ψ contain all the linear electrical and acoustic processes that are independent of the propagation in the sample and V_p and V_g are the phase and group velocities of the mode at frequency $\omega=\omega_0$.[32] In the general case, the condition for a particular zero crossing to occur in the received signal at distances x_0 and $x_0+\Delta x$ can be written as

$$\begin{aligned} R(x_0,t_0)&=R(x_0+\Delta x,t_0+\Delta t)\\ &=\frac{\partial R(x,t)}{\partial t}\,\Delta t+\frac{\partial R(x,t)}{\partial x}\,\Delta x, \end{aligned} \tag{A3}$$

where the partial derivatives are evaluated at $x=x_0$ and $t=t_0$. So, for the particular received signal expressed in Eq. (A2), the ratio of the distance difference to the zero crossing time difference is then

$$\frac{\Delta x}{\Delta t}=-\frac{\dfrac{\partial R(x,t)}{\partial t}}{\dfrac{\partial R(x,t)}{\partial x}}=\frac{f'\left(t-\dfrac{x}{V_g}\right)\cos\left[\omega_0\left(t-\dfrac{x}{V_p}\right)+\psi\right]-\omega_0 f\left(t-\dfrac{x}{V_g}\right)\sin\left[\omega_0\left(t-\dfrac{x}{V_p}\right)+\psi\right]}{\dfrac{1}{V_g}f'\left(t-\dfrac{x}{V_g}\right)\cos\left[\omega_0\left(t-\dfrac{x}{V_p}\right)+\psi\right]-\dfrac{\omega_0}{V_p}f\left(t-\dfrac{x}{V_g}\right)\sin\left[\omega_0\left(t-\dfrac{x}{V_p}\right)+\psi\right]}, \tag{A4}$$

where prime notation indicates differentiation with respect to the argument and it is assumed that the received signal remains the same. Equation (A4) indicates that the velocity measured by tracking a particular zero crossing in the received signal at two transducer–receiver spacings has some dependence on the group velocity as well as the phase velocity of the propagating mode at the center frequency, if the envelope signal has a finite derivative at the time of zero crossing. Hence, the condition for measurements sensitive only to phase velocity can be stated as

$$f'\left(t-\frac{x}{V_g}\right)=0 \quad \text{at } x=x_0, t=t_0 \Rightarrow V_p=\frac{\Delta x}{\Delta t}=V_p, \tag{A5}$$

which is satisfied by using gated long tone bursts as excitation signals.

APPENDIX B: ESTIMATION OF DIFFRACTION ERRORS IN LAMB WAVE PHASE VELOCITY MEASUREMENTS BY HERTZIAN CONTACT TRANSDUCERS

The diffraction error in determining the phase velocity of Lamb waves results from the finite size of the transmitter and receiver Hertzian contacts. This error can be considered an equivalent distance shift.[33] Considering Lamb wave propagation in an isotropic plate as a 2-D scalar wave, in a time harmonic case with $\exp(-j\omega t)$ variation, the field gen-

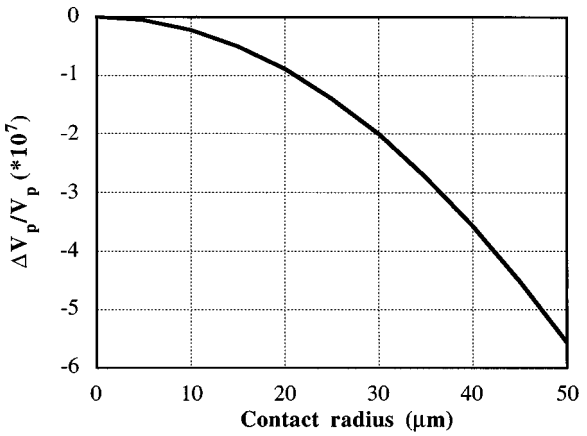

FIG. B1. The normalized phase velocity error due to diffraction as a function of Hertzian contact radius. The error scales with the square of the contact radius.

erated by an infinitesimally small cylindrical source at a distance r in the far field can be approximated as[34]

$$H_0^{(1)}(kr) \approx C\sqrt{2/\pi kr}\,\exp(jkr), \quad r > 3\lambda, \tag{B1}$$

where $H_0^{(1)}(\ )$ is the zeroth-order Hankel function, k is the wave number, λ is the wavelength, and C is a complex constant. The Hertzian contact transmitting transducer can be approximated as a source with uniform amplitude over a circular region of radius a, which is much smaller than the extensional wavelength in the buffer rod. To consider the worst case, we assume an infinitesimally small receiver. Then, the field at a distance r_1 from the origin, where the contact is centered, can be written as

$$I(r_1,a) \cong C\sqrt{\frac{2}{\pi k r_1}} \int_0^{2\pi}\int_0^a \exp(jkd(r_1,\rho,\phi))\rho\; d\rho\; d\phi, \tag{B2}$$

where ρ and ϕ are the source coordinates and $d(r_1,\rho,\phi)$ is the distance between the points $(r_1,0)$ and (ρ,ϕ). Noting that the phase velocity is determined by measuring the time delay at distances r_1 and r_2, the equivalent distance error due to diffraction is

$$\Delta r_i = \frac{1}{k}\left[\angle I(r_i,a) - \angle\exp(jkr_i)\right], \quad i = 1,2 \tag{B3}$$

for each measurement, where $\angle$ denotes the phase in radians. Then the resulting error in phase velocity measurement will be

$$\frac{\Delta V_p}{V_p} = \frac{\Delta r_2 - \Delta r_1}{r_2 - r_1}. \tag{B4}$$

In Fig. B1, the diffraction error in phase velocity measurement is plotted as a function of the Hertzian contact radius for a typical case of a Lamb wave excited in a 0.28-mm silicon wafer at 200 kHz, with $r_1 = 2.5$ cm and $r_2 = 2.7$ cm, which justifies the approximation in Eq. (B1).

[1] A. G. Every and W. Sachse, "Determination of elastic constants of anisotropic solids form acoustic-wave group-velocity data," Phys. Rev. B **42** (13), 8192–8204 (1990).

[2] B. Castagnede, J. T. Jenkins, W. Sachse, and S. Baste, "Optimal determination of the elastic constants of composite materials from ultrasonic wave-speed measurements," J. Appl. Phys. **67** (6), 2753–2761 (1990).

[3] B. D. Davidson, J. E. Michaels, V. Sundararaman, and T. E. Michaels, "Ultrasonic imaging of impact damaged composite panels," *Proceedings of the 1993 IEEE Ultrasonics Symposium* (IEEE, New York, 1993).

[4] A. Nayfeh and D. E. Chimenti, "Propagation of guided waves in fluid-coupled plates of fiber-reinforced composite," J. Acoust. Soc. Am. **83**, 1736–1743 (1988).

[5] D. E. Chimenti and A. Nayfeh, "Ultrasonic reflection and guided wave propagation in biaxially laminated composite plates," J. Acoust. Soc. Am. **87**, 1409–1415 (1990).

[6] R. B. Mignogna, N. K. Batra, and K. E. Simmonds, "Determination of elastic constants of anisotropic materials from oblique angle ultrasonic wave measurements II: Experimental," *Review of QNDE*, edited by D. O. Thompson and D. E. Chimenti (Plenum, New York, 1991), Vol. 10B, pp. 1677–1684.

[7] D. E. Chimenti, "Ultrasonic plate wave evaluation of composite laminates," *Proceedings of the 1991 IEEE Ultrasonics Symposium* (IEEE, New York, 1991), Vol. 2, pp. 863–71.

[8] D. A. Hutchins and A. C. Tam, "Pulsed photoacoustic materials characterization," IEEE Trans. Ultrason. Ferroelectr. Frequency Control **33**, 429–449 (1986).

[9] J. P. Monchalin, "Optical detection of ultrasound," IEEE Trans. Ultrason. Ferroelectr. Frequency Control **33**, 485–499 (1986).

[10] H. Sontag and A. C. Tam, "Optical detection of nanosecond acoustic pulses," IEEE Trans. Ultrason. Ferroelectr. Frequency Control **33**, 500–506 (1986).

[11] A. Cand, J.-P. Monchalin, and X. Jia, "Detection of in-plane and out-of-plane ultrasonic displacements by a two channel confocal Fabry–Perot interferometer," Appl. Phys. Lett. **64**, 414–416 (1994).

[12] J. I. Burov, K. P. Branzalov, and D. V. Ivanov "High accuracy noncontact laser-optical method for measuring surface acoustic wave velocity and attenuation," Appl. Phys. Lett. **46**, 141–142 (1985)

[13] C. Corbel, F. Guillois, D. Royer, M. Fink, and R. De Mol, "Laser generated elastic waves in carbon–epoxy composites," IEEE Trans. Ultrason. Ferroelectr. Frequency Control **40** (6), 710–716 (1993).

[14] D. W. Schindel, D. A. Hutchins, S. T. Smith, and B. Farahbakhsh, "High-temperature pulsed photoacoustic studies of surface waves on solids," J. Acoust. Soc. Am. **95**, 2517–2524 (1994).

[15] C. P. Hsieh and B. T. Khuri-Yakub, "One-point contact measurement of spherical resonances," Appl. Phys. Lett. **62**, 3091–3093 (1993).

[16] K. Y. Kim and W. Sachse, "Some novel applications of point source and point detector for ultrasonic waves," *Proceedings of the 1992 IEEE Ultrasonics Symposium* (IEEE, New York, 1992), Vol. 2, pp. 1009–1013.

[17] K. Y. Kim, W. Sachse, and A. G. Every, "On the determination of sound speeds in cubic crystals and isotropic media using a broadband ultrasonic point-source/point-receiver method," J. Acoust. Soc. Am. **93**, 1393–1406 (1993).

[18] D. B. Patterson, A. A. Godil, G. S. Kino, and B. T. Khuri-Yakub, "Acousto-optic modulators for optical fibers using Hertzian contact with a grooved transducer substrate," *Proceedings of the 1988 IEEE Ultrasonics Symposium* (IEEE, New York, 1988), Vol. 1, pp. 413–416.

[19] L. D. Landau and E. M. Lifshitz, *Theory of Elasticity* (Pergamon, New York, 1959), pp. 31–36.

[20] I. A. Victorov, *Rayleigh and Lamb Waves Physical Theory and Applications* (Plenum, New York, 1967).

[21] B. A. Auld, *Acoustic Fields and Waves in Solids* (Wiley, New York, 1973), Vol. 1.

[22] G. W. Farnell and E. L. Adler, "Elastic wave propagation in thin layers," in *Physical Acoustics*, edited by W. P. Mason and R. N. Thurston (Academic, New York, 1972), Vol. 9, pp. 76–88.

[23] M. R. Karim and A. K. Mal, "Inversion of leaky Lamb wave data by simplex algorithm," J. Acoust. Soc. Am. **88**, 482–491 (1990).

[24] F. E. Stanke and R. M. D'Angelo, "Clock and trigger jitter: effects on ultrasonic spectroscopy," *Proceedings of the 1988 IEEE Ultrasonics Symposium* (IEEE, New York, 1988), Vol. 2, pp. 873–878.

[25] W. Karunasena, A. H. Shah, and S. K. Datta, "Ultrasonic characterization of multilayered thick composite plates," *Review of QNDE*, edited by D. O. Thompson and D. E. Chimenti (Plenum, New York, 1991), Vol. 10B, pp. 1631–1637.

[26] J. J. Hall, "Electronic effects in the elastic constants of *n*-type silicon," Phys. Rev. **161** (1), 756–761 (1967).

[27] G. Simmons and H. Wang, *Single Crystal Elastic Constants and Calculated Aggregate Properties: A Handbook* (MIT, Cambridge, MA, 1971).

[28] The stiffness constants used for a uniaxial composite: c_{11}=141.85, c_{12}=4.38, c_{22}=10.72, c_{23}=4.37, c_{66}=5.38 in GPa.
[29] D. E. Chimenti and R. W. Martin, ''Nondestructive evaluation of composite laminates by leaky Lamb waves,'' Ultrasonics **29**, 13–21 (1991).
[30] The stiffness constants used for Teflon: c_{11}=3.88, c_{44}=0.65 in GPa. Density=2160 kg/m^3.
[31] A. M. Braga, ''Wave propagation in anisotropic layered composites,'' Ph.D. thesis, Stanford University, 1990.
[32] W. B. Jones, Jr., *Introduction to Optical Fiber Communication Systems* (Holt, Rinehart and Winston, Orlando, FL, 1988), pp. 45–48.
[33] J.-D. Aussel and J.-P. Monchalin, ''Precision laser-ultrasonic velocity measurement and elastic constant determination,'' Ultrasonics **27**, 165–177 (1989).
[34] K. Graff, *Wave Motion in Elastic Solids* (Dover, New York, 1991), p. 111.